



# Production of biologically active peptides by hydrolysis of whey protein isolates using hydrodynamic cavitation

Abhijeet Bhimrao Muley<sup>a,\*</sup>, Aniruddha Bhalchandra Pandit<sup>b</sup>, Rekha Satishchandra Singhal<sup>a</sup>, Sunil Govind Dalvi<sup>c</sup>

<sup>a</sup> Food Engineering and Technology Department, Institute of Chemical Technology, Matunga, Mumbai 400019, India

<sup>b</sup> Chemical Engineering Department, Institute of Chemical Technology, Matunga, Mumbai 400019, India

<sup>c</sup> Tissue Culture Section, Vasantdada Sugar Institute, Manjari (Bk.), Pune 412307, India

## ARTICLE INFO

### Keywords:

Whey protein isolate  
Hydrolysis  
Hydrodynamic cavitation  
Full factorial design  
Antioxidant properties  
Sugarcane *in vitro* growth

## ABSTRACT

Whey protein isolate (WPI) hydrolysates have higher solubility in aqueous phase and enhanced biological properties. Hydrolysis of WPI was optimized using operating pressure ( $\Delta P$ , bar), number of passes (N), and WPI concentration (C, %) as deciding parameters in hydrodynamic cavitation treatment. The optimum conditions for generation of WPI hydrolysate with full factorial design were 8 bar, 28 passes, and 4.5% WPI concentration yielding  $32.69 \pm 1.22$  mg/mL soluble proteins. WPI hydrolysate showed alterations in binding capacity over WPI. SDS-PAGE and particle size analysis confirmed the hydrolysis of WPI. Spectroscopic, thermal and crystallinity analyses showed typical properties of proteins with slight variations after hydrodynamic cavitation treatment. ABTS, DPPH and FRAP assays of WPI hydrolysate showed 7–66, 9–149, and 0.038–0.272  $\mu\text{mol/mL}$  GAE at 1–10, 0.25–4, and 3–30 mg/mL concentration, respectively. Further, a considerable enhancement in fresh weight, chlorophyll, carotenoids, reducing sugars, total soluble sugars, soluble proteins content and total phenolics content was noticed during *in vitro* growth of sugarcane in WPI hydrolysate supplemented medium at 50–200 mg/L concentration over the control. The process cost (INR/kg) to hydrolyze WPI was also calculated.

## 1. Introduction

Whey protein isolate (WPI), a byproduct of dairy product processing has gained popularity as an active and functional ingredient in food and pharmaceutical formulations. Due to production in huge quantities, it is available in abundance for different application such as stabilizers, foaming agents, gelling agents, and/or emulsifiers in food [1,2]. WPI are mainly composed of glycomacropeptide,  $\alpha$ -lactalbumin,  $\beta$ -lactoglobulin, bovine serum albumin, immunoglobulins, lactoperoxidase, proteose peptone and lactoferrin [3]. The essential amino acids present in WPI are valine, leucine, isoleucine, cysteine, phenylalanine, lysine, histidine, phenylalanine and tryptophan, which act as vital component for various metabolic pathways and functions in cells [4]. WPI displays many functional properties that are associated with their physicochemical properties in liquid medium. Solubility of WPI is of prime importance as other functional properties are significantly affected by it [5].

Majority of investigations on proteins for their properties have been reported on the native protein molecules but not on their hydrolysates

[3]. The hydrolysates are peptide/s and/or chains of amino acids which are reported to possess enhanced biological properties such as antioxidant, angiotensin-I converting enzyme inhibitory, plant growth promoting, anti-hypertensive and antimicrobial activities, among many others [6]. The overall antioxidant activity of protein hydrolysates is augmented as its tertiary and quaternary structure is broken down and the accessibility of released peptide/s and/or chains of amino acids in the medium is improved [7]. As compared to native protein molecules, these biologically active peptides not only have simple structure and low molecular weight, but can be easily absorbed by cells [8]. The application of protein hydrolysates through different means such as foliar application and/or fortification in growth medium have shown to trigger plant growth [9]. The growth is enhanced by stimulatory effect of hydrolyzed proteins triggering different metabolic pathways governing growth and development of plant by inducing seed germination, root and shoot development, and antimicrobial properties [10].

Proteins can be efficiently hydrolyzed by acid, alkaline, thermal, and enzymatic treatment, either individually or in combination. Hydrolysis

\* Corresponding author.

E-mail addresses: [abhijeetmuleypatil@gmail.com](mailto:abhijeetmuleypatil@gmail.com), [ft15ab.muley@pg.ictmumbai.edu.in](mailto:ft15ab.muley@pg.ictmumbai.edu.in) (A. Bhimrao Muley).

<https://doi.org/10.1016/j.ultsonch.2020.105385>

Received 5 April 2020; Received in revised form 27 September 2020; Accepted 29 October 2020

Available online 12 November 2020

1350-4177/© 2020 The Author(s).

Published by Elsevier B.V. This is an open access article under the CC BY-NC-ND license

(<http://creativecommons.org/licenses/by-nc-nd/4.0/>).

of proteins with acid and alkaline treatments have constraints of high amount of acid and alkali, complexities in handling due to high operating temperature and pressure, and need of their recovery [11]. Enzymatic hydrolysis is an environmental friendly approach, but it also has limitations of high processing cost and time of hydrolysis [12]. Cavitation mediated hydrolysis of WPI can be carried out at room temperature in aqueous solvents, and at ambient operating temperature and pressure conditions. Nowadays, hydrodynamic cavitation is emerging as a novel, non-thermal, energy efficient and green approach for different applications in food industries [13].

During cavitation, the generation and vicious collapse of bubbles (cavities) in liquid medium produce high pressure (approximately  $10^3$  bar) and high temperature (approximately  $10^4$  K) conditions releasing a huge amount of energy ( $1-10^{18}$  kW/m<sup>3</sup>) in a small instance of time [14]. These generated conditions trigger physical and chemical effects. The chemical effects cause decomposition of water molecules at the specified temperature and pressure condition leading to the generation of free radicals e.g. hydroxyl. The physical effect like turbulence is also produced after the liquid circulation [15]. Previously, different proteins such as keratin [11], peanut milk protein [16], and soy protein isolate [17] have been successfully degraded and/or hydrolyzed by the application of hydrodynamic cavitation under different set of optimized conditions.

The optimization of process parameters associated with hydrodynamic cavitation can be attained with either one variable at a time approach or mathematical modeling approach. Although one variable at a time approach is simple to perform, but the relationships amongst the interactions terms existing between the operating parameters cannot be enumerated. Mathematical modeling by response surface methodology is an effective statistical tool that has been applied in several fields for optimization of different processes [18]. Further, the impact of principle governing parameters and their possible interaction on the process can be effectively determined. Amongst the various available designs in mathematical modeling such as central composite and Box-Behnken, the full factorial design considers the effect of all possible combinations of variables at every possible combination level. It also requires the maximum number of experiments and thus create most reliable empirical model [19].

There are several reports on studies of acoustic cavitation and/or ultrasonic treatment of WPI for enhancement of structural and functional properties. However, very less literature is available on hydrolysis of WPI by hydrodynamic cavitation, its characterization and application. Therefore, the present study was undertaken to prepare biologically active peptides by hydrolysis of WPI using hydrodynamic cavitation as novel and green approach. To the best of our knowledge, this is the first report on optimization of hydrolysis of WPI by hydrodynamic cavitation using full factorial design, and then investigating its structural, thermal, and crystallinity properties. The antioxidant activities were evaluated using ABTS, DPPH and FRAP assays. Additionally, the *in vitro* growth promoting ability of WPI hydrolysates in sugarcane plant was assessed for the first time. Finally, the process cost in INR/kg associated with hydrolysis of WPI at varying pressure and different passes was also determined.

## 2. Materials and methods

### 2.1. Materials

Whey protein isolate was a gift sample from Cherish Pharma, Nashik, India. The *in vitro* sugarcane plants (*Saccharum officinarum* L. Co 86032) were provided by Tissue Culture Laboratory, VSI, Manjari (Bk.), Pune. Edible sunflower oil was purchased from local super market, Mumbai, India. All the media components were procured from Himedia Laboratories Pvt. Ltd. Mumbai, India, while other chemicals and reagents used in the work were of high purity, analytical grade and purchased from reliable sources.

### 2.2. Solubility of WPI

The insoluble matter content (%) was determined by a method explained by Muley et al. [20] with slight modifications. WPI (1 g) was mixed in 100 mL phosphate buffer (100 mM, pH 8.0) into a pre-weighed centrifuge tube and then continuously stirred at 140–150 rpm for 30 min. This solution was centrifuged for 10 min at  $7,195 \times g$  and  $25 \pm 2$  °C and the supernatant was decanted. The pellet so obtained was dried at  $60 \pm 2$  °C for 24 h and the insoluble matter content (%) was calculated as given in equation (1)

$$\text{Insoluble matter content (\%)} = \frac{\text{Initial WPI content} - \text{dissolved WPI content}}{\text{Initial WPI content}} \times 100 \quad (1)$$

### 2.3. Optimization of process parameters for hydrolysis of protein

The hydrolysis of WPI was done by using hydrodynamic cavitation and the approach used for optimization of process parameters associated with hydrolysis was full factorial design. The hydrodynamic cavitation reactor (Hycra Technologies Pvt. Ltd., Mumbai, India) had a venturi throat of 5 mm diameter, a 0.5 hp pump, a storage tank of 2 L volume, and could be operated at a maximum pressure of 12 bar and a maximum flow rate of 600 L/h. The schematic representation of hydrodynamic cavitation reactor set-up used in the study is illustrated in Fig. 1.

#### 2.3.1. Selection of range of process variables

The preliminary studies indicated the solubility of protein to be  $23.56 \pm 1.3\%$  and the soluble protein content to be  $2.46 \pm 0.32$  mg/mL at 1% concentration in phosphate buffer (100 mM, pH 8.0). The soluble protein content increased to  $8.32 \pm 0.21$ ,  $9.25 \pm 0.22$ ,  $11.15 \pm 0.13$  and  $12.31 \pm 0.17$  mg/mL after hydrodynamic cavitation treatment at 5, 6, 7 and 8 bar after 30 passes at 1.5% WPI concentration, respectively. Therefore, the lower limit or minimum requirement for the hydrolysis of protein was 5 bar/5 passes/1.5% WPI concentration. Table 1 illustrates the independent variables for the full factorial design. The upper limit for number of passes was set to 30 since more than 35 passes was considered to render the process economically unfeasible. The upper

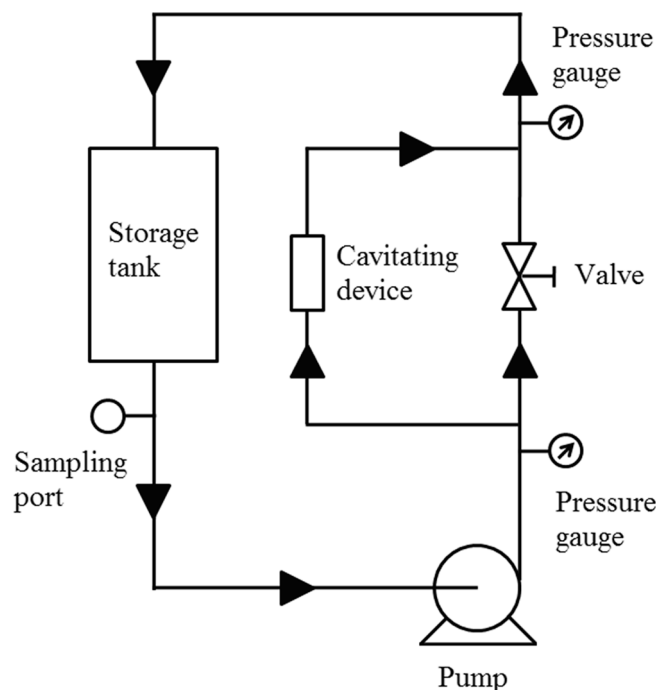


Fig. 1. Schematic representation of hydrodynamic cavitation reactor set-up.

**Table 1**  
Independent variables for full factorial design.

Independent variables	Symbol	Coded variable levels		
		Lower limit (-1)	Mid level (0)	Upper limit (1)
Operating pressure ( $\Delta P$ , bar)	$X_1$	4	6.5	8
Number of passes (N)	$X_2$	0	15	30
WPI concentration (C, %)	$X_3$	1.5	3.0	4.5

limit for the protein content was set at 4.5% due to the formation of a thick slurry above 4.5% which hindered the cavitation process itself.

### 2.3.2. Experimental design

Full factorial design with 3 independent variables namely operating pressure ( $\Delta P$ , bar), number of passes (N) and WPI concentration (C, %) were used to generate a quadratic polynomial model, as expressed in equation (2)

$$Y = \beta_0 + \beta_1 X_1 + \beta_2 X_2 + \beta_3 X_3 + \beta_4 X_1^2 + \beta_5 X_2^2 + \beta_6 X_3^2 + \beta_7 X_1 X_2 + \beta_8 X_2 X_3 + \beta_9 X_3 X_1 \quad (2)$$

where Y is the response, soluble protein content (SP, mg/mL),  $\beta_0$  to  $\beta_9$  are the regression coefficients,  $X_1$ ,  $X_2$  and  $X_3$  are the dimensionless coded values for  $\Delta P$ , N and C, respectively.

In the polynomial model, the real values were expressed in terms of coded values (as expressed in Equation (3) to (5)) to elucidate the relative importance of the individual process parameters and the terms (linear, interaction, and quadratic) affecting the response

$$X_1 = \left( \frac{\Delta P - 6.5}{1.5} \right) \quad (3)$$

$$X_2 = \left( \frac{N - 15}{15} \right) \quad (4)$$

$$X_3 = \left( \frac{C - 3}{1.5} \right) \quad (5)$$

After the full factorial design, a set of 84 experimental runs (Table 2) were carried out and one response, soluble protein content (SP, mg/mL), was determined.

### 2.3.3. Degree of hydrolysis

The degree of hydrolysis (DH) of WPI after hydrodynamic cavitation was determined by trichloroacetic acid (TCA) method explained by Hoyle and Merritt [21]. Briefly, hydrolyzed protein samples (1 mL) were thoroughly mixed with 20% TCA solution (1 mL) and incubated for 30 min. TCA precipitates the unhydrolyzed protein molecules (fragments of high molecular weight) that are present in the solution. This solution was centrifuged at  $7195 \times g$  for 5 min at  $25 \pm 2$  °C and the protein content of supernatant was measured by using Lowry et al. [22] assay with bovine serum albumin (0–500  $\mu\text{g/mL}$ ) as a standard protein. The DH (%) was determined as given in equation (6)

$$\text{DH}(\%) = \frac{\text{Soluble protein content in 20\% TCA (mg)}}{\text{Total protein content (mg)}} \times 100 \quad (6)$$

### 2.4. Binding capacity

The fat binding capacity and water binding capacity of WPI and WPI hydrolysate were determined as per protocol described by Muley et al.

[23].

## 2.5. Characterization of WPI and hydrolyzed WPI

### 2.5.1. Particle size analysis

The average particle size of insoluble fractions of WPI and hydrolyzed WPI was measured from mean particle size distribution on dynamic light scattering method on DLS Nanobrook 90 plus PALS, New York.

### 2.5.2. SDS-PAGE analysis

The changes in molecular weight of proteins in WPI after hydrodynamic cavitation were determined by SDS-PAGE. Electrophoresis was carried out using a stacking gel of 4% (pH 6.8) and 12% resolving gel (pH 8.8). The gel was run at a constant voltage (150 V) for 4 h at  $24 \pm 2$  °C using Bio-Rad, Mini-Protean®3 Tetra cell electrophoresis system (Bio-Rad, Richmond, CA, USA). The bands were visualized by staining with silver staining method by incubating the gel in 2% silver nitrate solution for exactly 25 min, which was further developed in 3% sodium carbonate and 0.5% formaldehyde.

### 2.5.3. Colour analysis

The colour of WPI and hydrolyzed WPI was measured by determining  $L^*$ ,  $a^*$  and  $b^*$  values using Hunter Lab (model DP-9000 D25 Hunter Associates Laboratory, Reston, VA, USA). The whiteness index was calculated as

$$\text{Whiteness index} = 100 - \sqrt{(100 - L^*)^2 + a^{*2} + b^{*2}} \quad (7)$$

### 2.5.4. Spectroscopic analysis

The  $\lambda_{\text{max}}$  of WPI and hydrolyzed WPI was determined on an UV-Vis spectrophotometer (UV 1800 Shimadzu, Japan).

### 2.5.5. FTIR analysis

The functional and characteristic peaks of WPI and hydrolyzed WPI were determined by using ATR spectrophotometer in the range 3800–500  $\text{cm}^{-1}$  (Bruker Corporations, Germany).

### 2.5.6. Secondary structure

The fractions of secondary structure in WPI and WPI hydrolysate were enumerated from FTIR. The secondary derivative of amide-I region (1700–1600  $\text{cm}^{-1}$ ) were recognized and then smoothened with Savitzky-Golay function in Essential FTIR™ 3.00. Finally, the quantify multi-component peak fitting program was applied under the amide-I domains of WPI and WPI hydrolysate to enumerate the fractions of secondary structures with the Gaussian function in Origin 8.5.

### 2.5.7. DSC and TGA analysis

The thermal stability of WPI and hydrolyzed WPI was measured with DSC (DSC-60 TA instrument, Shimadzu Corporation, Japan) and TGA (TGA-60H Shimadzu, Japan).

### 2.5.8. XRD analysis

The XRD pattern of WPI and hydrolyzed WPI was analyzed on a continuous scan mode X ray diffractometer coupled with Cu-K  $\alpha$ -radiation source (Lab X, XRD 6100, Shimadzu, Japan) and  $2\theta$  data collected between 10 and 80° at 1.2°/min step size.

## 2.6. Determination of biological properties of WPI hydrolysates

### 2.6.1. Antioxidant properties

The antioxidant activity of hydrolyzed WPI solution was estimated by using DPPH and ABTS assays at 1–10 mg/mL and 0.25–4.0 mg/mL, while the reducing capacity with FRAP assay at 3–30 mg/mL, respectively. The DPPH, ABTS and FRAP assays were carried out using a

Table 2

Combined hydrodynamic cavitation parameters according to full factorial design and the corresponding response as soluble protein content with corresponding degree of hydrolysis.

$\Delta P$ (bar)	Passes	WPI concentration (%)	$X_1$	$X_2$	$X_3$	$X_1X_1$	$X_2X_2$	$X_3X_3$	$X_1X_2$	$X_2X_3$	$X_3X_1$	Soluble proteins content (mg/mL)	Degree of hydrolysis (%)
5	0	1.5	-1	-1	-1	1	1	1	1	1	1	3.76 ± 0.41	27.26 ± 1.28
5	5	1.5	-1	-0.67	-1	1	0.44	1	0.67	0.67	1	4.21 ± 0.37	30.51 ± 1.35
5	10	1.5	-1	-0.33	-1	1	0.11	1	0.33	0.33	1	4.98 ± 0.36	36.09 ± 1.08
5	15	1.5	-1	0	-1	1	0	1	0	0	1	6.02 ± 0.37	43.62 ± 1.98
5	20	1.5	-1	0.33	-1	1	0.11	1	-0.33	-0.33	1	6.89 ± 0.40	49.93 ± 1.86
5	25	1.5	-1	0.67	-1	1	0.44	1	-0.67	-0.67	1	7.54 ± 0.45	54.64 ± 1.59
5	30	1.5	-1	1	-1	1	1	1	-1	-1	1	8.32 ± 0.55	60.29 ± 2.15
6	0	1.5	-0.33	-1	-1	0.11	1	1	0.33	1	0.33	3.76 ± 0.41	27.26 ± 1.28
6	5	1.5	-0.33	-0.67	-1	0.11	0.44	1	0.22	0.67	0.33	4.8 ± 0.44	34.78 ± 1.86
6	10	1.5	-0.33	-0.33	-1	0.11	0.11	1	0.11	0.33	0.33	5.35 ± 0.42	38.77 ± 1.98
6	15	1.5	-0.33	0	-1	0.11	0	1	0	0	0.33	6.58 ± 0.43	47.68 ± 2.18
6	20	1.5	-0.33	0.33	-1	0.11	0.11	1	-0.11	-0.33	0.33	7.44 ± 0.40	53.91 ± 2.64
6	25	1.5	-0.33	0.67	-1	0.11	0.44	1	-0.22	-0.67	0.33	8.05 ± 0.47	58.33 ± 3.06
6	30	1.5	-0.33	1	-1	0.11	1	1	-0.33	-1	0.33	9.25 ± 0.55	67.02 ± 2.66
7	0	1.5	0.33	-1	-1	0.11	1	1	-0.33	1	-0.33	3.76 ± 0.41	27.26 ± 1.28
7	5	1.5	0.33	-0.67	-1	0.11	0.44	1	-0.22	0.67	-0.33	5.39 ± 0.46	39.06 ± 1.98
7	10	1.5	0.33	-0.33	-1	0.11	0.11	1	-0.11	0.33	-0.33	6.27 ± 0.43	45.43 ± 1.31
7	15	1.5	0.33	0	-1	0.11	0	1	0	0	-0.33	7.45 ± 0.41	53.99 ± 1.24
7	20	1.5	0.33	0.33	-1	0.11	0.11	1	0.11	-0.33	-0.33	9.1 ± 0.43	65.94 ± 2.21
7	25	1.5	0.33	0.67	-1	0.11	0.44	1	0.22	-0.67	-0.33	10.35 ± 0.47	75.00 ± 2.45
7	30	1.5	0.33	1	-1	0.11	1	1	0.33	-1	-0.33	11.15 ± 0.55	80.80 ± 2.61
8	0	1.5	1	-1	-1	1	1	1	-1	1	-1	3.76 ± 0.41	27.26 ± 1.28
8	5	1.5	1	-0.67	-1	1	0.44	1	-0.67	0.67	-1	6.12 ± 0.53	44.35 ± 1.63
8	10	1.5	1	-0.33	-1	1	0.11	1	-0.33	0.33	-1	7.46 ± 0.49	54.06 ± 1.69
8	15	1.5	1	0	-1	1	0	1	0	0	-1	8.63 ± 0.48	62.54 ± 1.28
8	20	1.5	1	0.33	-1	1	0.11	1	0.33	-0.33	-1	12.02 ± 0.49	87.10 ± 2.34
8	25	1.5	1	0.67	-1	1	0.44	1	0.67	-0.67	-1	12.23 ± 0.53	88.62 ± 2.50
8	30	1.5	1	1	-1	1	1	1	1	-1	-1	12.31 ± 0.62	89.20 ± 2.46
5	0	3	-1	-1	0	1	1	0	1	0	0	7.82 ± 0.37	28.33 ± 1.17
5	5	3	-1	-0.67	0	1	0.44	0	0.67	0	0	9.58 ± 0.31	34.71 ± 1.22
5	10	3	-1	-0.33	0	1	0.11	0	0.33	0	0	10.95 ± 0.30	39.67 ± 1.40
5	15	3	-1	0	0	1	0	0	0	0	0	12.76 ± 0.32	46.23 ± 1.65
5	20	3	-1	0.33	0	1	0.11	0	-0.33	0	0	13.83 ± 0.33	50.11 ± 1.78
5	25	3	-1	0.67	0	1	0.44	0	-0.67	0	0	14.11 ± 0.38	51.12 ± 1.56
5	30	3	-1	1	0	1	1	0	-1	0	0	14.29 ± 0.48	51.77 ± 1.44
6	0	3	-0.33	-1	0	0.11	1	0	0.33	0	0	7.82 ± 0.37	28.33 ± 1.17
6	5	3	-0.33	-0.67	0	0.11	0.44	0	0.22	0	0	14.48 ± 0.36	52.46 ± 1.36
6	10	3	-0.33	-0.33	0	0.11	0.11	0	0.11	0	0	15.05 ± 0.31	54.53 ± 1.51
6	15	3	-0.33	0	0	0.11	0	0	0	0	0	15.85 ± 0.30	57.43 ± 1.80
6	20	3	-0.33	0.33	0	0.11	0.11	0	-0.11	0	0	16.61 ± 0.32	60.18 ± 1.72
6	25	3	-0.33	0.67	0	0.11	0.44	0	-0.22	0	0	16.85 ± 0.38	61.05 ± 2.01
6	30	3	-0.33	1	0	0.11	1	0	-0.33	0	0	17.02 ± 0.50	61.67 ± 1.58
7	0	3	0.33	-1	0	0.11	1	0	-0.33	0	0	7.82 ± 0.37	28.33 ± 1.17
7	5	3	0.33	-0.67	0	0.11	0.44	0	-0.22	0	0	15.3 ± 0.38	55.43 ± 1.48
7	10	3	0.33	-0.33	0	0.11	0.11	0	-0.11	0	0	16.42 ± 0.32	59.49 ± 2.12
7	15	3	0.33	0	0	0.11	0	0	0	0	0	17.51 ± 0.30	63.44 ± 2.60
7	20	3	0.33	0.33	0	0.11	0.11	0	0.11	0	0	17.85 ± 0.31	64.67 ± 2.11
7	25	3	0.33	0.67	0	0.11	0.44	0	0.22	0	0	18.03 ± 0.36	65.33 ± 2.66
7	30	3	0.33	1	0	0.11	1	0	0.33	0	0	18.27 ± 0.47	66.19 ± 2.74
8	0	3	1	-1	0	1	1	0	-1	0	0	7.82 ± 0.37	28.33 ± 1.17
8	5	3	1	-0.67	0	1	0.44	0	-0.67	0	0	16.26 ± 0.55	58.91 ± 2.86
8	10	3	1	-0.33	0	1	0.11	0	-0.33	0	0	17.32 ± 0.50	62.75 ± 2.59
8	15	3	1	0	0	1	0	0	0	0	0	18.05 ± 0.48	65.40 ± 2.48
8	20	3	1	0.33	0	1	0.11	0	0.33	0	0	18.35 ± 0.47	66.48 ± 1.88
8	25	3	1	0.67	0	1	0.44	0	0.67	0	0	19.05 ± 0.49	69.02 ± 2.32
8	30	3	1	1	0	1	1	0	1	0	0	19.49 ± 0.55	70.61 ± 2.84
5	0	4.5	-1	-1	1	1	1	1	1	-1	-1	11.4 ± 0.41	27.54 ± 1.84
5	5	4.5	-1	-0.67	1	1	0.44	1	0.67	-0.67	-1	18.04 ± 0.32	43.57 ± 2.20
5	10	4.5	-1	-0.33	1	1	0.11	1	0.33	-0.33	-1	18.69 ± 0.28	45.14 ± 1.48
5	15	4.5	-1	0	1	1	0	1	0	0	-1	19.55 ± 0.27	47.22 ± 1.52
5	20	4.5	-1	0.33	1	1	0.11	1	-0.33	0.33	-1	20.02 ± 0.28	48.36 ± 2.16
5	25	4.5	-1	0.67	1	1	0.44	1	-0.67	0.67	-1	20.58 ± 0.28	49.71 ± 2.35
5	30	4.5	-1	1	1	1	1	1	-1	1	-1	21.1 ± 0.32	50.97 ± 2.11
6	0	4.5	-0.33	-1	1	0.11	1	1	0.33	-1	-0.33	11.4 ± 0.41	27.54 ± 1.84
6	5	4.5	-0.33	-0.67	1	0.11	0.44	1	0.22	-0.67	-0.33	19.67 ± 0.59	47.51 ± 2.38
6	10	4.5	-0.33	-0.33	1	0.11	0.11	1	0.11	-0.33	-0.33	20.55 ± 0.55	49.64 ± 2.17
6	15	4.5	-0.33	0	1	0.11	0	1	0	0	-0.33	21.99 ± 0.52	53.11 ± 2.54
6	20	4.5	-0.33	0.33	1	0.11	0.11	1	-0.11	0.33	-0.33	23.32 ± 0.51	56.33 ± 3.01
6	25	4.5	-0.33	0.67	1	0.11	0.44	1	-0.22	0.67	-0.33	23.83 ± 0.52	57.56 ± 2.97
6	30	4.5	-0.33	1	1	0.11	1	1	-0.33	1	-0.33	24.02 ± 0.57	58.02 ± 1.53
7	0	4.5	0.33	-1	1	0.11	1	1	-0.33	-1	0.33	11.4 ± 0.41	27.54 ± 1.84
7	5	4.5	0.33	-0.67	1	0.11	0.44	1	-0.22	-0.67	0.33	27.19 ± 0.61	65.68 ± 2.56

(continued on next page)

Table 2 (continued)

$\Delta P$ (bar)	Passes	WPI concentration (%)	$X_1$	$X_2$	$X_3$	$X_1X_1$	$X_2X_2$	$X_3X_3$	$X_1X_2$	$X_2X_3$	$X_3X_1$	Soluble proteins content (mg/mL)	Degree of hydrolysis (%)
7	10	4.5	0.33	-0.33	1	0.11	0.11	1	-0.11	-0.33	0.33	27.48 ± 0.56	66.38 ± 3.45
7	15	4.5	0.33	0	1	0.11	0	1	0	0	0.33	28.15 ± 0.53	67.99 ± 1.48
7	20	4.5	0.33	0.33	1	0.11	0.11	1	0.11	0.33	0.33	28.98 ± 0.41	70.00 ± 2.52
7	25	4.5	0.33	0.67	1	0.11	0.44	1	0.22	0.67	0.33	29.64 ± 0.49	71.59 ± 1.94
7	30	4.5	0.33	1	1	0.11	1	1	0.33	1	0.33	30.02 ± 0.40	72.51 ± 2.64
8	0	4.5	1	-1	1	1	1	1	-1	-1	1	11.4 ± 0.41	27.54 ± 1.84
8	5	4.5	1	-0.67	1	1	0.44	1	-0.67	-0.67	1	25.09 ± 1.21	60.60 ± 2.35
8	10	4.5	1	-0.33	1	1	0.11	1	-0.33	-0.33	1	27.58 ± 0.37	66.62 ± 3.64
8	15	4.5	1	0	1	1	0	1	0	0	1	30.58 ± 1.11	73.86 ± 2.45
8	20	4.5	1	0.33	1	1	0.11	1	0.33	0.33	1	31.98 ± 0.72	77.25 ± 1.98
8	25	4.5	1	0.67	1	1	0.44	1	0.67	0.67	1	32.58 ± 1.08	78.70 ± 2.23
8	30	4.5	1	1	1	1	1	1	1	1	1	32.69 ± 0.59	78.96 ± 2.18

modified method explained by Vijayan et al. [24].

### 2.6.2. Growth promoting properties

The growth promoting ability of soluble fractions of hydrolyzed WPI solution was determined on *in vitro* growth of sugarcane plants by adding them in MS medium at varying concentrations (0, 50, 100, 150 and 200 mg/L) before autoclaving. The growth medium without soluble fractions of hydrolyzed WPI was used as a control. The respective growth media (40 mL) was inoculated with sugarcane explants and incubated at  $25 \pm 2$  °C with continuous shaking at 80–90 rpm. The change in plant fresh weight and biochemical parameters like chlorophyll (a, b and total), carotenoids, reducing sugars, soluble proteins and phenolics content was measured after 23–24 days of incubation to determine the plant growth.

### 2.7. Statistical analysis

All the experiments were performed in triplicates and analyzed in duplicate, and the results were documented as arithmetic mean  $\pm$  standard deviation. The data was analyzed with Microsoft Excel (2010) and SPSS (Version16). One way ANOVA was applied to check the mean and statistical significance amongst the values obtained with the Duncan's New Multiple Range test at confidence interval 95%.

## 3. Results and discussion

### 3.1. Solubility of WPI

WPI was partially soluble in water with a percent insoluble content of  $76.46 \pm 0.18\%$  and the soluble protein content of  $2.46 \pm 0.32$  mg/mL

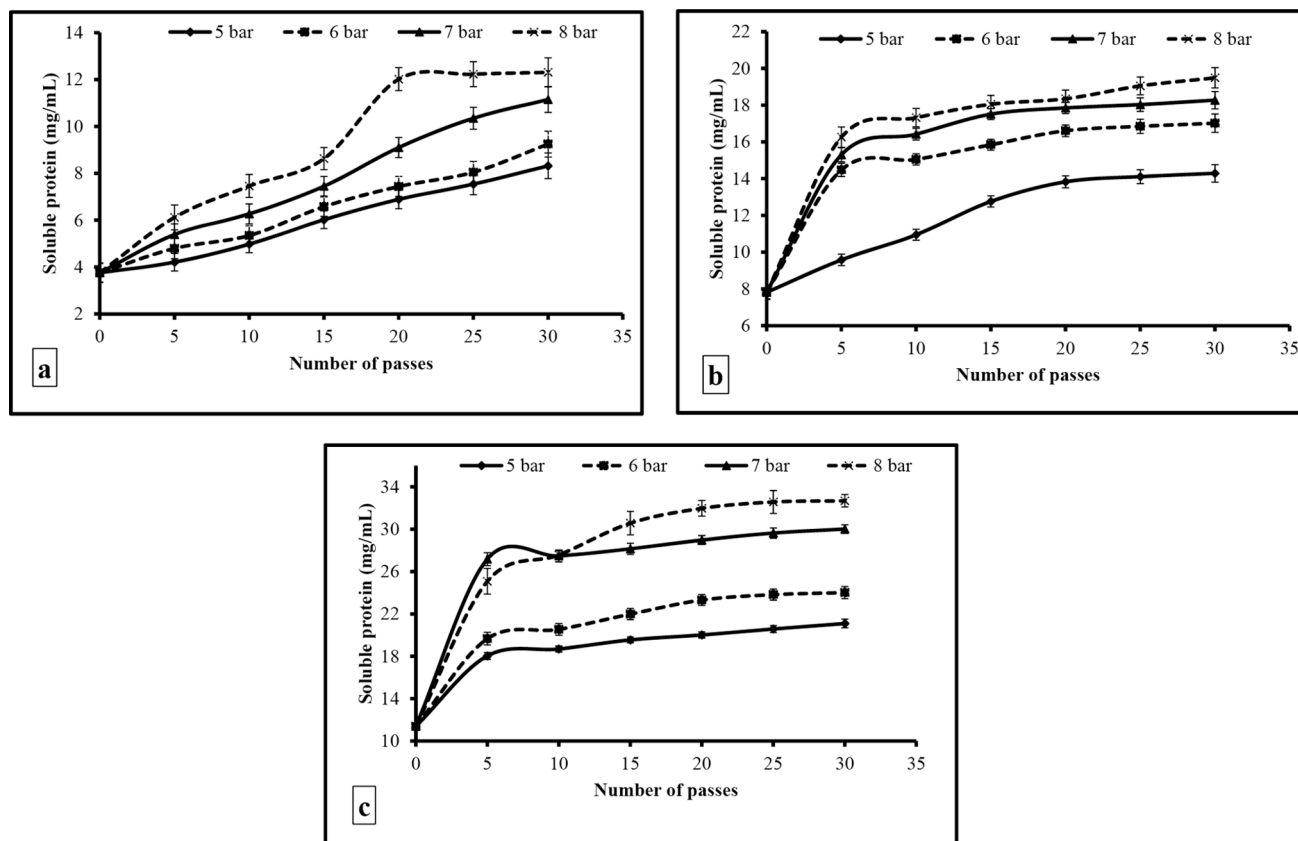


Fig. 2. Effect of operating pressure and number of passes on the hydrolysis of WPI at (a) 1.5%, (b) 3.0%, and (c) 4.5% protein concentration.



at 1% WPI concentration, respectively. The solubility profile was also determined in a varying pH regime, and it was seen that solubility increased with increase in pH. Highest solubility was seen at pH 9.0. The solubility of protein is associated with different factors such as pH and temperature of the surrounding medium and structural conformation state (native or deformed). The pH of the medium has an influence on nature and distribution of the net charge on protein. Generally, proteins are highly soluble in high (alkaline) or low (acids) pH due to availability of excess charges of same sign, producing repulsion amongst the molecules, and thus contributing to higher solubility [5]. Additionally, the solubility of WPI in a solvent system is decided by the energy difference amongst the protein-protein interactions and protein-solvent interactions.

### 3.2. Effect of operating conditions on hydrolysis of WPI

The effect of operating pressure and number of passes on the formation of soluble proteins was studied at 1.5, 3.0, and 4.5% WPI concentration. There was an increase in the degree of hydrolysis of WPI (as estimated from the formation of soluble proteins) with an increase in operating pressure, number of passes, and WPI concentration (Fig. 2). After hydrodynamic cavitation at 5, 6, 7 and 8 bar, the soluble protein content increased to  $8.32 \pm 0.21$ ,  $9.25 \pm 0.22$ ,  $11.15 \pm 0.13$ , and  $12.31 \pm 0.17$  mg/mL after 30 passes at 1.5% WPI concentration, and this corresponded to  $60.29 \pm 2.15$ ,  $67.02 \pm 2.66$ ,  $80.80 \pm 2.61$ , and  $89.20 \pm 2.46$ % degree of hydrolysis, respectively. The amount of soluble proteins formed at 3% and 4.5% WPI concentration were  $14.29 \pm 0.18$ ,  $17.02 \pm 0.24$ ,  $18.27 \pm 0.19$ , and  $19.49 \pm 0.26$ ;  $21.1 \pm 0.11$ ,  $24.02 \pm 0.17$ ,  $30.02 \pm 0.22$ , and  $32.69 \pm 0.25$  after 30 passes and at 5, 6, 7 and 8 bar, and this corresponded to  $51.77 \pm 1.44$ ,  $61.67 \pm 1.58$ ,  $66.19 \pm 2.74$ , and  $70.61 \pm 2.84$ %; and  $50.97 \pm 2.11$ ,  $58.02 \pm 1.53$ ,  $72.51 \pm 2.64$ , and  $78.96 \pm 2.18$ % degree of hydrolysis, respectively. There was a sudden rise in soluble protein content and degree of hydrolysis of WPI between 10 and 15 passes followed by a gradual increase. The soluble protein  $2.46 \pm$

$$Y = 16.54 + 2.88X_1 + 4.46X_2 + 7.96X_3 - 0.43X_1^2 - 3.36X_2^2 + 0.41X_3^2 + 1.40X_1X_2 + 1.41X_2X_3 + 1.66X_3X_1 \quad (8)$$

0.32 mg/mL at 1% WPI concentration which is already present in WPI might have also contributed to the soluble protein content. WPI might have got broken down into smaller particles or fragments during the early cycles (passes) of cavitation and with subsequent cycles these hydrolyzed particles along with the WPI particles might have again got hydrolyzed, and led to production of soluble proteins.

The hydrolysis of WPI may be due to the action of shear forces formed by the shock waves after consequent formation and collapse of cavities. These cavities produce high temperature and pressure states liberating a huge amount of energy in a due course of time [26]. The turbulence, shear stresses and collapse pressure in combination with the formed free radicals effectively breaks down the protein particles and facilitate the formation of WPI hydrolysates [11,14].

### 3.3. Optimization of hydrolysis of WPI by full factorial design

A full factorial design with three variables viz. operating pressure, number of passes and WPI concentration was employed to achieve maximum soluble protein content (mg/mL). In full factorial design, the range of each variable was transformed into coded value, and labeled as +1 (upper limit), 0 (mid level), and -1 (lower limit), respectively (Table 1). A total set of 84 experimental conditions were suggested by full factorial design which consisted of linear, square and interaction terms. The hydrolysis of WPI was measured in terms of formation of soluble proteins formed and were significantly affected by operating

process parameters of hydrodynamic cavitation ( $\Delta P$ , N and C; Table 2). The interaction amongst the variables operating pressure ( $X_1$ ), number of passes ( $X_2$ ), and WPI concentration ( $X_3$ ), against a single response i.e. the generation of soluble proteins (Y) was enumerated with the linear, quadratic polynomial, and cubic models, respectively. The adequacy of the model was set by considering all the experimental conditions with a minimum deviation, along with the significant *F* and *p*-value. The interaction amongst the variables demonstrated excellent relationship with quadratic polynomial model, which was highlighted from higher  $R^2$  (0.946) and adjusted  $R^2$  (0.940) values. The linear model and cubic model did not produce good fit, and further resulted in higher noise. The efficient adequacy of the developed model was seen from the lower *p*-value ( $<0.0001$ ) and higher *F*-value (145.13). In the modeling associated with response surfaces, it is important to achieve higher *F*-value as it facilitates in the rejection of null hypothesis, and further distinguishes the components based on the average values [18]. The effect of varying operating pressure, number of passes, and WPI concentration on the degree of hydrolysis of WPI or soluble proteins formed was calculated as coefficient estimates (Table 3).

The hydrolysis of WPI was considerably affected by the three linear interaction terms, and all the three parameters produced positive coefficients. The formation of protein hydrolysates was influenced by WPI concentration (7.96), number of passes (4.46), and operating pressure (2.88) (Table 3). Further, a synergistic effect (positive effect) was seen amongst the square terms WPI concentration (1.66), operating pressure (1.40), and number of passes (1.14) on the formation of protein hydrolysates as they signified positive values. In the interaction terms, antagonist effect (negative effect) was observed between operating pressure and number of passes (-0.43), and number of passes and WPI concentration (-3.36), while synergistic effect (positive effect) between operating pressure and WPI concentration (0.41).

The quadratic polynomial equation was developed by investigating the experimental data in triplicates

where Y is the soluble proteins formed after hydrodynamic cavitation, whereas  $X_1$ ,  $X_2$ , and  $X_3$  are the coded values of test variables viz. operating pressure, number of passes and WPI concentration, respectively.

The interaction amongst the operating pressure and number of passes, number of passes and WPI concentration, and operating pressure and WPI concentration during the optimization hydrolysis of WPI are shown in the Fig. 3a, Fig. 3b and Fig. 3c, respectively. The interactions

**Table 3**

Coefficients of all the terms in polynomial model and the corresponding ANOVA data indicating the effect of hydrodynamic cavitation operating parameters on degree of hydrolysis of WPI.

Component estimates	Pseudocoefficient estimates
Intercept	59.36
A	9.37
B	16.90
C	2.53
A <sup>2</sup>	-1.94
B <sup>2</sup>	-10.45
C <sup>2</sup>	-0.19
AB	4.02
BC	-3.43
AC	1.77
p-Model	<0.0001
F-Model	66.68
R <sup>2</sup>	0.890
Adj R <sup>2</sup>	0.877

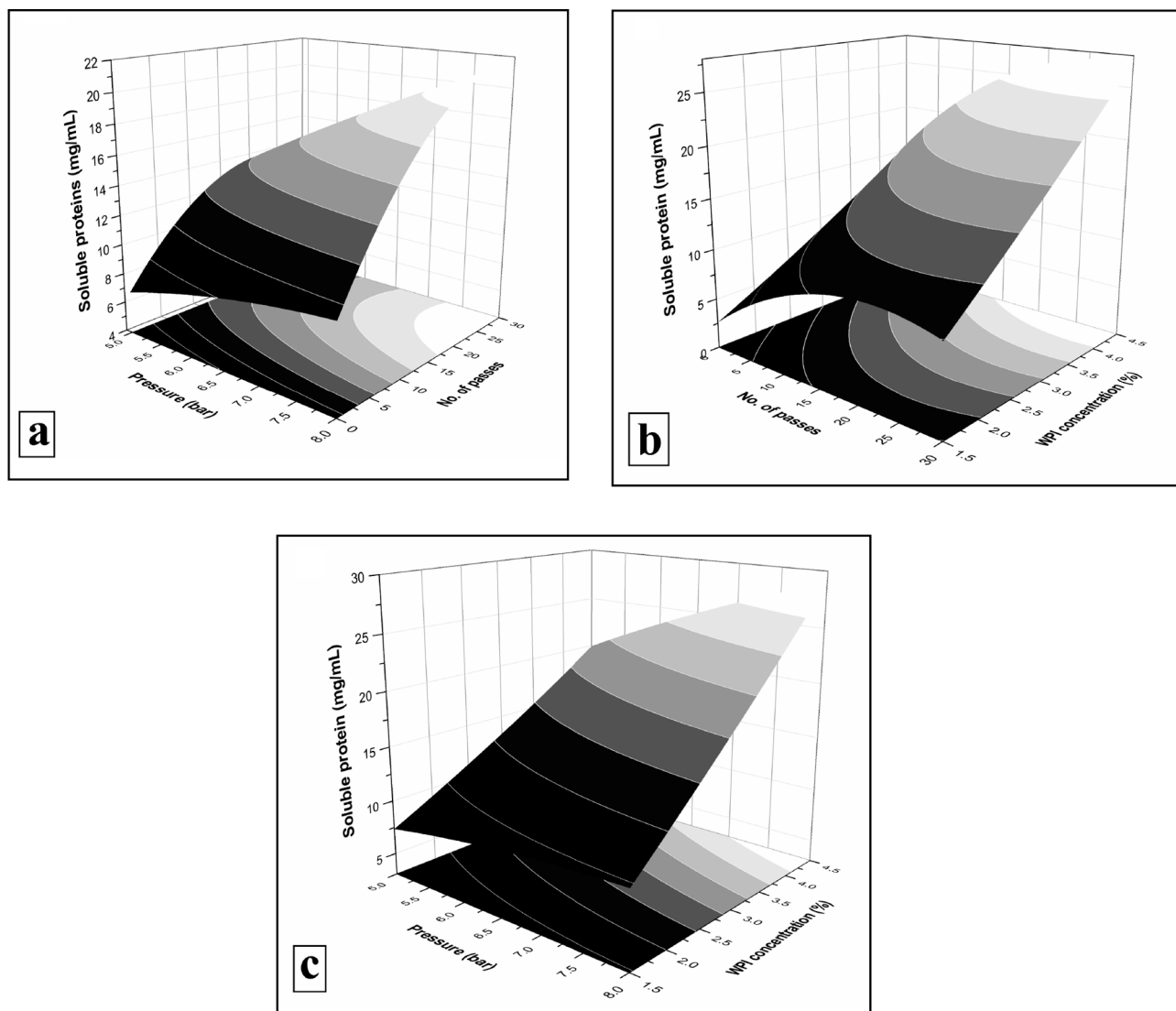


Fig. 3. Surface response plots (2D and 3D) for interaction of (a) operating pressure and number of passes, (b) number of passes and WPI concentration, and (c) operating pressure and WPI concentration during the optimization hydrolysis of WPI.

amongst the corresponding values were significant, and the shape of 3D surface response and 2D contour plot was concave in nature. The conditions fixed for desirability values of the numerical statistical optimization procedure were '4 + importance' and 'in range' for pressure and number of passes, while '2 + importance' and 'minimum' for WPI concentration to achieve '3 + importance' with 'maximum' soluble protein content and 0.93 desirability (Table 4). The optimal process conditions for soluble protein content were extracted from the Design Expert Software. The maximum soluble proteins ( $32.69 \pm 0.81$  mg/mL) were formed at 8 bar operating pressure, with 28 passes and at 4.5% WPI concentration.

The validation of the developed model was confirmed

experimentally by attaining the process conditions equivalent to maximum soluble proteins, and were then correlated with the achieved experimental values. The obtained optimum process conditions after statistical optimization (8 bar/28 passes/4.5% WPI concentration) were studied again and the amount of soluble proteins obtained was  $32.15 \pm 0.62$  mg/mL. This obtained value was in close correlation with the value attained from optimized process conditions.

#### 3.4. Binding capacities

The capability of protein isolates to hold, absorb and retain water and/or oil is an important aspect for development of food and/or

Table 4

Set of constraints for operating parameters targeting hydrolysis of WPI through the combined hydrodynamic cavitation operating parameters.

Rank	Pressure (bar)	Number of passes	WPI concentration (%)	Soluble protein (mg/mL)	Desirability
Pre-setting goal	In range	In range	Minimize	Maximize	NA
Pre-setting importance	4+	4+	2+	3+	3+
1	8	28	4.5	32.64	0.93
2	8	26	4.5	32.60	0.92
3	8	30	4.5	32.68	0.92
4	8	25	4.5	32.58	0.91
5	8	24	4.5	31.42	0.89

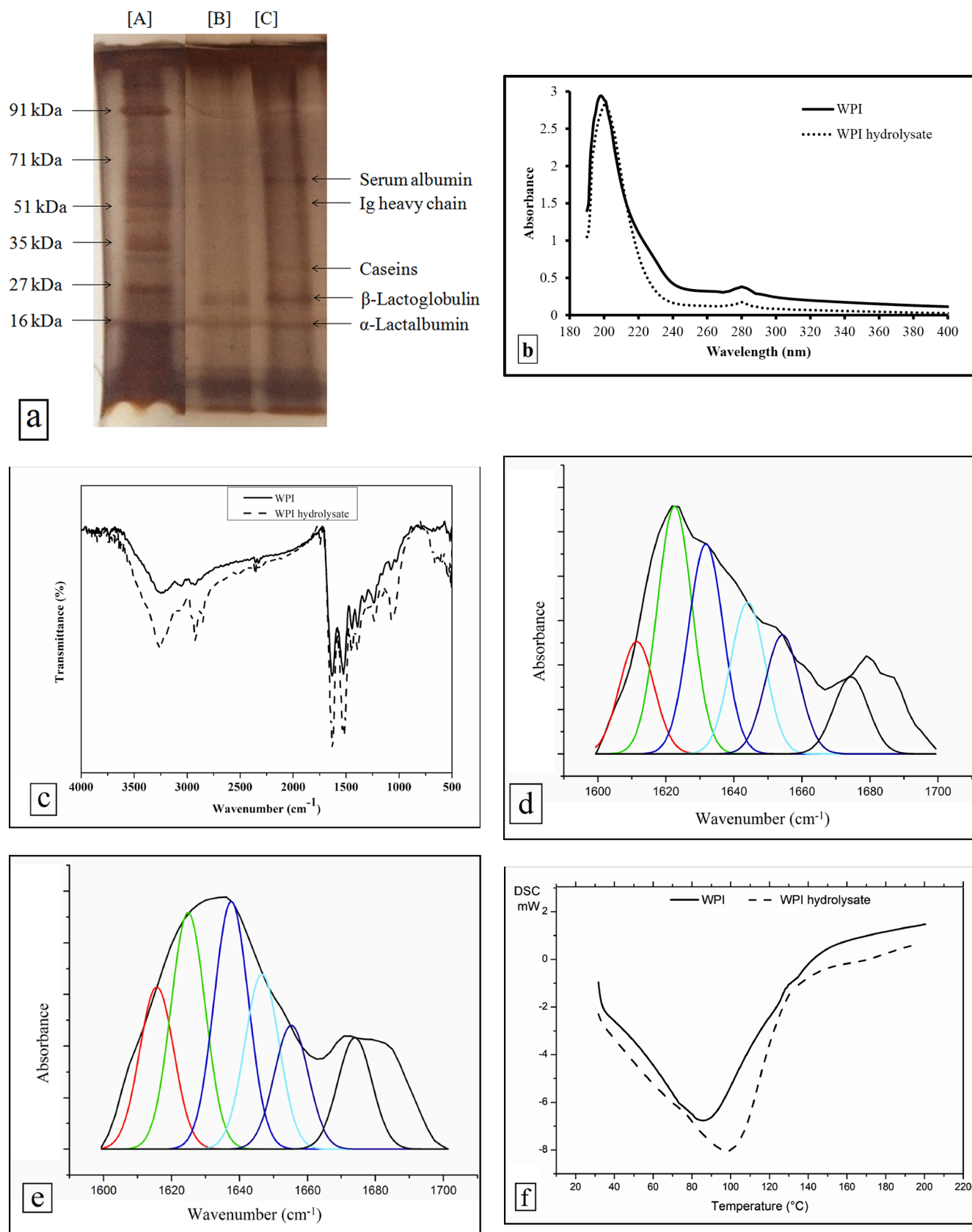


**Fig. 4.** (a). SDS-PAGE profile of WPI and WPI hydrolysate [Lane A: standard molecular weight markers, Lane B: WPI hydrolysate, and Lane C: WPI]; (b) UV-Vis spectra of WPI and WPI hydrolysate; (c) FTIR spectra of WPI and WPI hydrolysate; secondary structure analysis of (d) WPI and (e) WPI hydrolysate as determined by Gaussian multi-component fitting [The secondary structure fractions:  $\beta$ -antiparallel (red colour),  $\beta$ -strands (green colour),  $\beta$ -sheets (blue colour), random coils (cyan colour),  $\alpha$ -helices (navy blue colour) and  $\beta$ -turns (black colour)]; (f) DSC profile of WPI and WPI hydrolysate; (g) TGA profile of WPI and WPI hydrolysate; and (h) XRD profile of WPI and WPI hydrolysate. (For interpretation of the references to colour in this figure legend, the reader is referred to the web version of this article.)



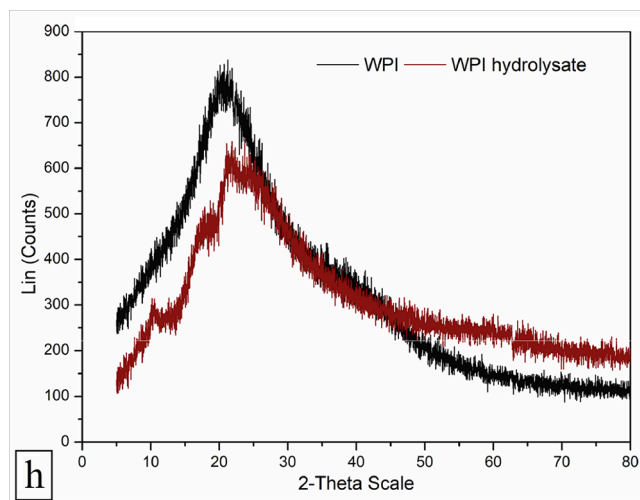
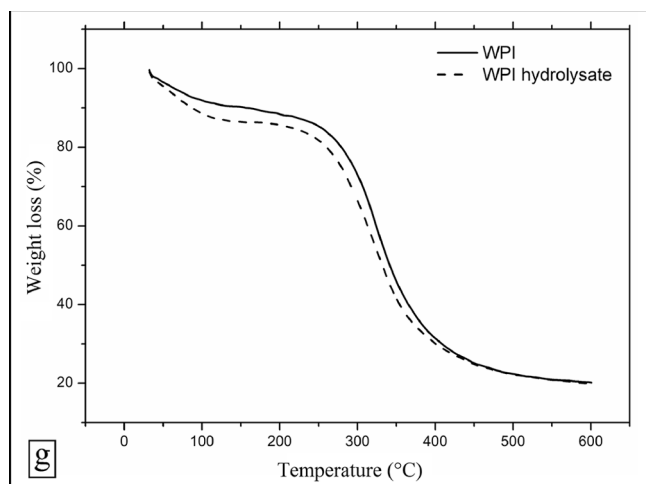


Fig. 4. (continued).

biological systems. The fat binding capacity of WPI and WPI hydrolysate was  $425.31 \pm 33.79\%$  and  $354.43 \pm 9.07\%$ , respectively. The water binding capacity of WPI was  $303.72 \pm 5.06\%$  while the determination of water binding capacity of WPI hydrolysate prepared by hydrodynamic cavitation treatment was not possible as they were completely soluble in water. The binding capacities of proteins are not only influenced by isolation technique, shape, size, surface hydrophobicity, non-polar side chains on surface, conformational characteristics, steric factors, but also its molecular weight [26].

### 3.5. Instrumental characterization

The characterization of WPI and WPI hydrolysate was performed with different instrumental analysis techniques to evaluate the changes occurred after hydrodynamic cavitation treatment. The instrumental characterization was done to determine the characteristic functional features and properties associated with them.

#### 3.5.1. Particle size analysis

The particle size was measured by dynamic light scattering method and the statistical diameter of WPI was 186.80 nm (Figure S1-a Supplementary file) which got reduced to 35.88 nm (Figure S1-b Supplementary file) after hydrodynamic cavitation treatment under optimum conditions. The reduction in size of WPI may be due to the shear forces generated by the shock waves after subsequent formation and then collapse of bubbles [25]. These shock waves gives mechanical (shear stresses, turbulences, and collapse pressure), thermal, and chemical (formation of free radicals) effects which may lead to breakdown of particles [11,14].

#### 3.5.2. SDS-PAGE analysis

The hydrolysis of WPI after hydrodynamic cavitation was monitored by SDS-PAGE. The electrophoretic pattern of the standard protein markers, prepared WPI hydrolysate, and WPI are shown in lane A, lane B, and lane C, respectively (Fig. 4a). WPI displayed the presence of whey proteins (Lane C) which included serum albumin (nearly 65–67 kDa), immunoglobulins (Ig, 58–62 kDa), caseins (nearly 28–30 kDa),  $\beta$ -lactoglobulin (nearly 18–20 kDa) and  $\alpha$ -lactalbumin (nearly 14–15 kDa). Hydrodynamic cavitation caused the hydrolysis of protein in WPI as confirmed from the disappearance of protein fractions of large molecular weight in the gel (Lane B). The fractions of nearly 18–20 kDa, 14–15 kDa, and smaller peptide fractions were seen after hydrodynamic cavitation (Lane B). These newly developed peptides and other degradation products could not be completely revealed by the SDS-PAGE analysis, the main reason being removal of amino acids and short

peptides (below 1 kDa) from the WPI hydrolysate during electrophoresis and/or the staining process.

#### 3.5.3. Colour analysis

The colour of WPI and WPI hydrolysate powder was estimated by using Hunter scale. The results indicated that the creamish yellow WPI became white after hydrodynamic cavitation treatment. The  $L^*$ ,  $a^*$  and  $b^*$  values of WPI and WPI hydrolysate were  $72.17 \pm 0.1$ ,  $13.88 \pm 0.1$  and  $45.22 \pm 0.35$ , and  $84.40 \pm 0.24$ ,  $1.11 \pm 0.10$  and  $19.37 \pm 0.38$ , respectively. The whiteness index of WPI increased from  $45.15 \pm 0.35$  to  $75.10 \pm 0.44$  after hydrodynamic cavitation treatment. The increase in whiteness index might be due to breakdown of pigments responsible for creamish yellow colouration of WPI.

#### 3.5.4. Spectroscopic analysis

The absorption spectra (UV–Vis) of WPI and WPI hydrolysate were studied in a range of 190 to 400 nm to determine the changes in  $\lambda_{\max}$  (Fig. 4b). It was seen that both WPI and WPI hydrolysate possessed nearly similar absorption spectra with a peaks at 200 and 280 nm. The peptide bonds are responsible for a sharp peak at 200 nm, while the amino acids with aromatic side chains accounts for peak at 280 nm [27]. Further, there might be breakdown and/or removal of aromatic amino acids from WPI after hydrodynamic cavitation as seen from reduced intensity of peak at 280 nm.

#### 3.5.5. FTIR analysis

The FTIR analysis of WPI and WPI hydrolysate was performed over a range 4000 to 500  $\text{cm}^{-1}$  to investigate the variations in the functional peaks. Both, WPI as well as WPI hydrolysates showcased distinctive spectra of a typical protein molecule (Fig. 4c). There was no major change in the FTIR spectra of WPI and WPI hydrolysate specifying that no functional groups were added after hydrodynamic cavitation treatment. The functional characteristic peaks in the 1700 to 1600  $\text{cm}^{-1}$ , 1500 to 1400  $\text{cm}^{-1}$ , and 3400 to 3300  $\text{cm}^{-1}$  regime not only signified the presence of amide I and amide II bands but also the presence of -OH stretching vibrations and/or -NH stretch, CO=NH linkages, and peptide linkages, respectively. Moreover, there was an increase in intensities of all the functional and characteristic peaks after hydrodynamic cavitation indicating the exposure of more functional groups due to hydrolysis of WPI.

#### 3.5.6. Secondary structure

The alterations that occurred in the fractions of secondary structure of WPI before and after hydrodynamic cavitation treatment were enumerated from the amide-I domain (1600–1700  $\text{cm}^{-1}$ ) of the FTIR

spectra. The quantitative estimation of fractions of secondary structure in WPI (Fig. 4d) and WPI hydrolysate (Fig. 4e) was carried out by Gaussian function using multi-peak curve fitting. There were significant changes in structural conformation of WPI after hydrodynamic cavitation as deduced from the second derivative. The fractions of  $\beta$ -antiparallel (red colour),  $\beta$ -strands (green colour),  $\beta$ -sheets (blue colour), random coils (cyan colour),  $\alpha$ -helix (navy blue colour) and  $\beta$ -turns (black colour) in WPI were 4.49, 32.02, 13.78, 16.78, 9.20, and 23.71%, and 23.57, 9.53, 23.46, 6.23, 2.78, and 34.43% in WPI hydrolysate, respectively. The changes in secondary structure fractions could be ascribed to both hydrolysis of WPI into smaller protein fractions caused by hydrodynamic cavitation, as well as changes occurring in the hydration layer as evidenced by the increased solubility in water.

### 3.5.7. DSC analysis

The DSC profile of WPI and WPI hydrolysate exhibited a decomposition pattern with two distinct steps (Fig. 4f). There was a considerable decline in the phase transition temperature of WPI after hydrolyzing with hydrodynamic cavitation. The first endothermic step initiated at 27.27 °C and 32.59 °C, and ended at 38.09 °C and 40.94 °C which signified moisture loss from WPI and WPI hydrolysate, respectively. The second endothermic step started at 28.78 °C and 30.92 °C, and ended at 123.29 °C and 127.77 °C and this corresponded to breakdown and decomposition of protein moieties in WPI and WPI hydrolysate, respectively. The cumulative enthalpies of both the peaks in WPI and WPI hydrolysate were  $-391.11$  J/g and  $-141.94$  J/g, respectively. This prominent decrease in enthalpy of WPI after hydrodynamic cavitation signified a reduction in energy of phase transition, and the plausible reason might be the reduced molecular weight.

### 3.5.8. TGA analysis

The TGA profile of WPI and WPI hydrolysate highlighted a two step decomposition pattern (Fig. 4g). The first decomposition step appeared between the temperature domain 60–190 °C, and a substantial weight loss of 10.44 and 13.73% for WPI and WPI hydrolysate was noticed at 170 °C and 160 °C, respectively. This decomposition stage can be corroborated with the loss of moisture that is bound with the protein molecules. The second decomposition step was seen in the temperature regime 250–450 °C, a considerable weight loss of 40.69 and 41.11% for WPI and WPI hydrolysate was noticed at 325.07 °C and 315.02 °C, respectively. This decomposition stage can be corroborated with breakdown of protein molecules. The change in maximum temperature by around 10 °C in both the decomposition steps after the hydrodynamic cavitation treatment of WPI could corroborated to hydrolysis of WPI. The thermal stability of WPI hydrolysates was lower than WPI due to breakdown of peptide bonds,  $\beta$ -sheets and non-covalent interactions holding protein molecules together [11]. The temperature at which 15, 30, 45, 60 and 75% weight loss occurred in WPI and WPI hydrolysate were also reported (Table 5). There was a total weight loss of around 79.83 and 80.11% in WPI and WPI hydrolysate with a further increase in temperature up to 600 °C. Further, the weight percentage of WPI and WPI hydrolysate left un-decomposed after TGA analysis at a temperature of 600 °C under nitrogen atmosphere was 20.17 and 19.89%.

**Table 5**  
TGA results of WPI and WPI hydrolysate.

Sample	T <sub>15</sub> (°C) <sup>a</sup>	T <sub>30</sub> (°C) <sup>b</sup>	T <sub>45</sub> (°C) <sup>c</sup>	T <sub>60</sub> (°C) <sup>d</sup>	T <sub>75</sub> (°C) <sup>e</sup>	Char Yield (%) <sup>f</sup>
WPI	252.84	306.61	332.27	365.46	451.53	20.17
WPI hydrolysate	214.74	291.72	322.25	354.01	447.19	19.89

<sup>a</sup> Temperature at which 15% weight loss was recorded by TGA at heating rate of 10 °C/min under nitrogen atmosphere.

<sup>b</sup> Temperature at which 30% weight loss was recorded by TGA at heating rate of 10 °C/min under nitrogen atmosphere.

<sup>c</sup> Temperature at which 45% weight loss was recorded by TGA at heating rate of 10 °C/min under nitrogen atmosphere.

<sup>d</sup> Temperature at which 60% weight loss was recorded by TGA at heating rate of 10 °C/min under nitrogen atmosphere.

<sup>e</sup> Temperature at which 75% weight loss was recorded by TGA at heating rate of 10 °C/min under nitrogen atmosphere.

<sup>f</sup> Weight percentage of material left un-decomposed after TGA analysis at a temperature of 600 °C under nitrogen atmosphere.

### 3.5.9. XRD analysis

The XRD profile was studied to evaluate the changes in crystallinity pattern of WPI before and after hydrodynamic cavitation treatment. Both WPI and WPI hydrolysate showed a single broad and distinctive peak at around 20° and 21°, respectively (Fig. 4h). Both WPI as well as WPI hydrolysate were amorphous in nature as confirmed from the large and broad nature of the functional peaks. The mass crystallinity (%) of WPI and WPI hydrolysate was 6.47% and 5.08% as enumerated from the ratio of the area of functional peak to the total area using Origin software (version 8.5). The peaks at  $2\theta$  values considered for the crystalline region of WPI and WPI hydrolysate were 20° and 23°, respectively. A shift in functional peak along with considerable reduction in the peak intensity after hydrodynamic cavitation implied a significant decline in the crystallinity of WPI.

The WPI hydrolysates were prepared and characterized using various instrumental techniques. Protein hydrolysates are known to possess different biological properties such as plant growth promotion, antioxidant, anti-inflammatory, antihypertensive, antimicrobial, and immunomodulatory properties, amongst many others. Here the antioxidant and growth promoting properties of the prepared WPI hydrolysates were studied.

### 3.6. Antioxidant capacities

Antioxidant activity is associated with the compounds and/or molecules that are capable of preventing a biologically active system against the prominently harmful impact of reactions and/or processes involving the formation of reactive nitrogen and oxygen species that cause excessive oxidation [28]. Different methods are used to assess the antioxidant capacities but it is generally recommended to carry two or more assays for determination of antioxidant activity as there are irregularities with different radicals. ABTS and DPPH assays detects the radical scavenging capacity, while FRAP assay measures the reducing capacity *i.e.* ferrous reducing activity.

The radical scavenging and reducing capacity mechanisms of the WPI hydrolysate could be related to pervasiveness of the hydrophobic amino acids such as alanine, proline, valine, isoleucine, leucine, phenylalanine, tryptophan, tyrosine and methionine [4]. The other amino acids that may also contribute in antioxidant activity are lysine, cysteine, and histidine [29]. In addition, the amino acids with aromatic side chains can also donate protons to the electron deficient radicals further improving the radical scavenging property. The antioxidant capacity of WPI hydrolysate was studied with the ABTS and DPPH radical scavenging assay, while the reducing capacity was analyzed by the FRAP assay. The results of the same are presented in Table 6.

The ABTS radical scavenging activity of WPI hydrolysate was seen at 0.25–4.0 mg/mL. An inhibition of  $5.63 \pm 1.15\%$  to  $87.01 \pm 1.12\%$  of ABTS radicals was noticed at 0.25 to 4.0 mg/mL WPI hydrolysate concentration which corresponded to  $9.65 \pm 1.14$   $\mu\text{mol/mL}$  to  $148.94 \pm 1.11$   $\mu\text{mol/mL}$  of gallic acid equivalent, respectively. WPI hydrolysate showed  $2.40 \pm 0.11\%$  to  $22.15 \pm 0.84\%$  inhibition of DPPH radicals at 1 to 10 mg/mL concentration and this was equivalent to  $7.05 \pm 0.32$   $\mu\text{mol/mL}$  to  $65.46 \pm 2.49$   $\mu\text{mol/mL}$  of gallic acid. At higher

**Table 6**  
Free radical scavenging activity and reducing capacity of WPI hydrolysate.

WPI hydrolysate (mg/mL)	DPPH ( $\mu\text{mol/mL}$ GAE)	WPI hydrolysate (mg/mL)	ABTS ( $\mu\text{mol/mL}$ GAE)	WPI hydrolysate (mg/mL)	FRAP ( $\mu\text{mol/mL}$ GAE)
1.0	7.05 $\pm$ 0.32	0.25	9.65 $\pm$ 1.14	3.0	0.038 $\pm$ 0.007
2.0	13.63 $\pm$ 0.64	0.50	27.39 $\pm$ 0.38	6.0	0.071 $\pm$ 0.009
3.0	21.40 $\pm$ 0.77	0.75	39.13 $\pm$ 1.71	9.0	0.098 $\pm$ 0.007
4.0	28.70 $\pm$ 0.71	1.0	48.72 $\pm$ 0.96	12.0	0.129 $\pm$ 0.003
5.0	35.63 $\pm$ 0.90	1.5	77.59 $\pm$ 1.59	15.0	0.164 $\pm$ 0.010
6.0	42.69 $\pm$ 0.83	2.0	104.44 $\pm$ 1.56	18.0	0.190 $\pm$ 0.004
7.0	49.49 $\pm$ 1.84	2.5	124.50 $\pm$ 0.97	21.0	0.218 $\pm$ 0.104
8.0	56.56 $\pm$ 0.91	3.0	133.78 $\pm$ 0.64	24.0	0.250 $\pm$ 0.006
9.0	63.12 $\pm$ 1.36	3.5	144.58 $\pm$ 0.95	27.0	0.266 $\pm$ 0.006
10.0	65.46 $\pm$ 2.49	4.0	148.94 $\pm$ 1.11	30.0	0.272 $\pm$ 0.003

concentration, precipitation of protein was seen as DPPH is soluble in methanol or ethanol [30]. The organic solvents are known to reduce the solubility of soluble proteins by removing the hydration layer around their vicinity. The variations in the inhibition of ABTS and DPPH radicals by WPI hydrolysate may be due to the medium in which assays were performed. ABTS was carried out in aqueous medium while DPPH in organic solvent. In addition, the difference in solubility and diffusivity of free radicals and even peptides in protein hydrolysate may have also contributed for the same [28].

During the FRAP assay, an increase in absorption from  $0.035 \pm 0.006$  to  $0.252 \pm 0.003$  was noticed which was equivalent to  $0.038 \pm 0.007$  to  $0.272 \pm 0.003$   $\mu\text{mol/mL}$  of gallic acid at 3 to 30 mg/mL concentration of WPI hydrolysate, respectively. The increase in absorption with increased protein concentration could be correlated to availability of more functional groups in protein hydrolysate for reduction of FRAP molecules from ferric ( $\text{Fe}^{3+}$ ) to ferrous ( $\text{Fe}^{2+}$ ) form [31]. Further, it has been found that due to proton donating ability, aspartic acid and glutamic acid are amongst the most potential contributors in FRAP assay. Additionally, due to sulphhydryl groups, cysteine and methionine contribute to strong reducing ability [32].

### 3.7. Supplementation of WPI hydrolysate for *in vitro* growth promotion in sugarcane plant

The growth promoting ability of WPI and WPI hydrolysate was determined by supplementing it at varying concentration (0, 50, 100,

150 and 200 mg/L) concentration in MS growth medium for *in vitro* growth of sugarcane plants. Precipitation was seen in the growth medium supplemented with different concentrations of WPI after autoclaving (Figure S2 to S4, Supplementary file). Further, the colour of the media was lighter while that of WPI was slightly darker. Although the main reason for this observation unclear, one plausible reason could be the binding of other nutrients with WPI. When sugarcane plantlets were inoculated the growth was completely abnormal and there was early death of plantlets. In addition, it was also very difficult to differentiate between the contaminated and normal tissue culture bottles due to appearance of similar turbidity pattern. Hence, the *in vitro* growth promotion in sugarcane plants was carried out with WPI hydrolysate.

The change in plant fresh weight and biochemical parameters of sugarcane plants such as chlorophyll (a, b and total), carotenoids, reducing sugars, soluble proteins, and total phenolics content associated with its growth were analyzed after 23–24 days of incubation (Table 7). There was a slight change in plant fresh weight after supplementing the growth medium with WPI hydrolysate. There was an increment in weight by 10.97, 4.66, 13.16 and 8.32% over the control after supplementing WPI hydrolysate at 50, 100, 150 and 200 mg/L concentration in MS growth medium, respectively. The slight increase in the biomass may be attributed to the ability of protein hydrolysates to promote nitrogen accumulation in the plant during growth via a coordinated regulation of nitrogen and carbon metabolic pathways [33]. The protein hydrolysates might have also enhanced the uptake of both micro and macronutrients and use them efficiently [34].

There was a marginal increase in the biochemical parameters with an increase in the concentration of WPI hydrolysate in the sugarcane growth medium, but significantly superior results were observed at 150 and 200 mg/L supplemented medium. In the plant system, the estimation of pigment content is an essential factor for determining the growth [35,36]. The pigments have dual functions viz. harvesting the light and scavenging the free oxygen radicals at abnormal irradiance levels [37]. The chlorophyll a, chlorophyll b and total chlorophyll content in the sugarcane leaves increased substantially by 1.80, 2.04 and 1.87 folds after the supplementation of 200 mg/L of WPI hydrolysate to the growth medium over the control. There was a slight increase in carotenoids content from  $0.19 \pm 0.05$  mg/g FW to  $0.25 \pm 0.03$  mg/g FW after incorporation of 150 mg/L WPI hydrolysate in the growth medium. The increase in pigment synthesis and compounds associated with it in response to protein hydrolysates can be attributed to plant hormones (auxins and gibberellins) activities [34].

There was a remarkable increase in the reducing sugars, total soluble sugars, soluble proteins and total phenolics by 1.28, 1.21, 1.34 and 1.35 times after the supplementation of WPI hydrolysate at 150 mg/L over the control, and the corresponding values were  $4.66 \pm 0.50$  mg/g FW,  $7.05 \pm 0.15$  mg/g FW,  $9.84 \pm 0.18$  mg/g FW, and  $0.42 \pm 0.01$  mg/g FW, respectively. The considerable improvement in growth of sugarcane plants after supplementation of WPI hydrolysate in plant growth medium indirectly enhanced the chances of harvesting excess light which further caused higher photosynthesis, and increased accumulation of

**Table 7**  
Effect of protein hydrolysate supplementation on biochemical parameters during *in vitro* growth of sugarcane plants.

Protein concentration (mg/L)	Plant fresh weight (g)	Chlorophyll a (mg/g FW)	Chlorophyll b (mg/g FW)	Total chlorophyll (mg/g FW)	Carotenoids (mg/g FW)	Reducing sugars (mg/g FW)	Total soluble sugars (mg/g FW)	Soluble proteins (mg/g FW)	Total phenolics content (mg/g FW)
0	10.94 $\pm$ 0.30 <sup>a</sup>	0.97 $\pm$ 0.21 <sup>c</sup>	0.50 $\pm$ 0.09 <sup>c</sup>	1.48 $\pm$ 0.30 <sup>c</sup>	0.19 $\pm$ 0.05 <sup>a</sup>	3.65 $\pm$ 0.15 <sup>c</sup>	5.81 $\pm$ 0.17 <sup>d</sup>	7.33 $\pm$ 0.45 <sup>c</sup>	0.31 $\pm$ 0.02 <sup>c</sup>
50	12.14 $\pm$ 0.38 <sup>a</sup>	1.44 $\pm$ 0.14 <sup>ab</sup>	0.73 $\pm$ 0.05 <sup>b</sup>	2.17 $\pm$ 0.18 <sup>ab</sup>	0.21 $\pm$ 0.04 <sup>a</sup>	4.30 $\pm$ 0.59 <sup>bc</sup>	6.49 $\pm$ 0.18 <sup>c</sup>	8.58 $\pm$ 0.44 <sup>b</sup>	0.35 $\pm$ 0.02 <sup>bc</sup>
100	11.45 $\pm$ 0.48 <sup>a</sup>	1.14 $\pm$ 0.21 <sup>b</sup>	0.64 $\pm$ 0.10 <sup>b</sup>	1.78 $\pm$ 0.3 <sup>b</sup>	0.23 $\pm$ 0.02 <sup>a</sup>	4.99 $\pm$ 0.09 <sup>a</sup>	6.78 $\pm$ 0.13 <sup>b</sup>	9.46 $\pm$ 0.59 <sup>a</sup>	0.39 $\pm$ 0.01 <sup>ab</sup>
150	12.38 $\pm$ 0.56 <sup>a</sup>	1.44 $\pm$ 0.16 <sup>ab</sup>	0.69 $\pm$ 0.12 <sup>b</sup>	2.13 $\pm$ 0.27 <sup>ab</sup>	0.25 $\pm$ 0.03 <sup>a</sup>	4.66 $\pm$ 0.50 <sup>ab</sup>	7.05 $\pm$ 0.15 <sup>a</sup>	9.84 $\pm$ 0.18 <sup>a</sup>	0.42 $\pm$ 0.01 <sup>a</sup>
200	11.85 $\pm$ 0.85 <sup>a</sup>	1.75 $\pm$ 0.14 <sup>a</sup>	1.02 $\pm$ 0.06 <sup>a</sup>	2.77 $\pm$ 0.19 <sup>a</sup>	0.23 $\pm$ 0.04 <sup>a</sup>	4.15 $\pm$ 0.14 <sup>bc</sup>	6.94 $\pm$ 0.18 <sup>ab</sup>	9.77 $\pm$ 0.30 <sup>a</sup>	0.41 $\pm$ 0.02 <sup>a</sup>

biomolecules such as proteins, sugars, carotenoids and phenolics. The probable reason for increased growth parameters could be the stimulatory effect of few peptides and amino acids in protein hydrolysates in triggering several metabolic pathways involved in growth and development of plant [33]. The soluble proteins, peptides and amino acids can be easily absorbed by the plant. The amino acids also have precise function in promoting the plant growth [38]. The presence of peptides and amino acids in protein hydrolysates could also act as surplus reservoir of nitrogen source in the medium during the growth of plant. Protein hydrolysates have also been previously reported to elicit the pathways for carbohydrate and amino acid metabolism [39]. Furthermore, it can also be hypothesized that the peptides and amino acids in protein hydrolysates supplemented in the medium might have provided carbon and nitrogen skeletons for conversions into precursors and/or intermediates in the metabolic pathways like tricarboxylic acid cycle. This might have further contributed in the respiratory metabolic pathways and ATP production during the energy associated processes such as transport of nutrients [40].

### 3.8. Estimation of power and cost for the process

The commercial feasibility of any process is dependent on the power and energy consumed, and the cost to run it. With an increase in the operating pressure, the power requirement also increases which significantly contribute to process cost required to operate the pump. In addition, process duration is also linked to operating time and this is associated with number of passes. Therefore the optimization of processing parameters such as pressure and number of passes is of prime importance. The expected cost for hydrolysis of WPI operated at different pressures and different passes was calculated. It was seen that the cost (INR/kg) required to hydrolyze 1 kg WPI at 4.5% WPI concentration was substantially less as compared to lower WPI concentrations (Table 8). The enumeration of power and costing is briefly elaborated below.

Sample calculation for required power and cost:

For processing 1.5% WPI solution and system operation at 5 bar for 20 passes

(1) Operating pressure =  $\Delta P = 5$  bar

$$\Delta P = 500 \text{ kPa}$$

(2) The time required to pass 10 L of 1.5% WPI solution was 34.51 sec

Therefore, the volumetric flow rate (Q):

$$Q = 10 \text{ L}/34.51 \text{ sec}$$

$$Q = 1.043 \text{ m}^3/\text{h}$$

(3) The working volume of was 1 L

Therefore, time required for 20 passes was 69.02 sec

Processing time (t):

$$t = 69.02 \text{ sec}$$

$$t = 19.172 \times 10^{-3} \text{ h}$$

(4) Power required for processing 1 m<sup>3</sup> of 1.5% WPI solution (P)

$$P = \Delta P \times Q \times t$$

$$P = 500 \times 1.043 \times 19.172 \times 10^{-3} \text{ kWh/m}^3$$

$$P = 10 \text{ kWh/m}^3$$

(5) Operating cost for processing 1 m<sup>3</sup> of 1.5% WPI solution (C)

$$C = P \times \text{cost of power}$$

$$C = 10 \times 7 \text{ (Considering 7 INR/kWh)}$$

**Table 8**

Process cost for hydrolysis of WPI at different operating pressures with different passes.

Protein concentration (%)	Number of passes	Cost (INR/kg of WPI)			
		5 Bar	6 Bar	7 Bar	8 Bar
1.5	10	2.33	2.80	3.27	3.73
	20	4.67	5.60	6.53	7.47
	30	7.00	8.40	9.8	11.20
3.0	10	1.17	1.40	1.63	1.86
	20	2.33	2.80	3.27	3.72
	30	3.50	4.21	4.9	5.58
4.5	10	0.78	0.93	1.09	1.24
	20	1.56	1.87	2.18	2.48
	30	2.33	2.80	3.27	3.72

$$C = 70 \text{ INR/m}^3$$

(6) Now, 1 m<sup>3</sup> WPI solution contains 15 kg of WPI

Therefore the operating cost (C)

$$C = 70/15 \text{ INR/kg}$$

$$C = 4.67 \text{ INR/kg}$$

The amount required to hydrolyze 1 kg WPI at 5 bar and 20 passes was 4.37 INR.

## 4. Conclusion

The present study suggests that hydrodynamic cavitation is an efficient technique for breakdown of WPI particles and subsequently hydrolyzing them into soluble fractions. The optimum conditions for hydrolysis of WPI as determined by full factorial design were 8 bar, 28 passes, and 4.5% WPI concentration which yielded  $32.69 \pm 1.22$  mg/mL soluble proteins. The prepared WPI hydrolysates possessed higher solubility in aqueous phase and enhanced biological properties. The native structure of WPI as deduced by UV-Vis and FTIR spectroscopy indicated maintenance of basic structure, while DSC, TGA and XRD analyses highlighted typical characteristics of proteins with slight variations after hydrodynamic cavitation treatment. The generated biological peptides possessed prominent antioxidant potential as enumerated from ABTS, DPPH and FRAP assays. Further, the supplementation of WPI hydrolysates in sugarcane growth medium at 50–200 mg/L considerably improved the fresh weight, chlorophyll, carotenoids, reducing sugars, total soluble sugars, soluble proteins content and total phenolics content as compared to the control. The process cost to hydrolyze WPI at higher WPI concentration, and different operating pressure and varying passes was lower than that compared at lower WPI concentration. The prepared WPI hydrolysates can be considered as bioactive molecules that can find different food, pharmaceutical and biotechnological applications.

## CRedit authorship contribution statement

**Abhijeet Bhimrao Muley:** Conceptualization, Data curation, Formal analysis, Investigation, Methodology, Project administration, Resources, Software, Validation, Visualization, Writing - original draft. **Aniruddha Bhalchandra Pandit:** Investigation, Project administration, Resources, Supervision, Visualization. **Rekha Satishchandra Singhal:** Conceptualization, Data curation, Formal analysis, Funding acquisition, Investigation, Project administration, Resources, Supervision, Validation, Visualization. **Sunil Govind Dalvi:** Investigation, Resources, Supervision, Visualization.

## Declaration of Competing Interest

The authors declare that they have no known competing financial interests or personal relationships that could have appeared to influence



the work reported in this paper.

## Acknowledgement

The authors are grateful to University Grants Commission, Government of India, for providing financial supports by awarding fellowship under BSR scheme (Award number: F.25-1/2014-15(BSR)/No.F.5-62/2007(BSR) dated 16<sup>th</sup> Feb 2015) to carry out this research work.

## Appendix A. Supplementary data

Supplementary data to this article can be found online at <https://doi.org/10.1016/j.ulsonch.2020.105385>.

## References

- [1] R. Adjonu, G. Doran, P. Torley, S. Agboola, Whey protein peptides as components of nanoemulsions: A review of emulsifying and biological functionalities, *J. Food Eng.* 122 (2014) 15–27, <https://doi.org/10.1016/j.jfoodeng.2013.08.034>.
- [2] K. Li, M.W. Woo, H. Patel, L. Metzger, C. Selomulya, Improvement of rheological and functional properties of milk protein concentrate by hydrodynamic cavitation, *J. Food Eng.* 221 (2018) 106–113, <https://doi.org/10.1016/j.jfoodeng.2017.10.005>.
- [3] R.J.S. de Castro, M.A.F. Domingues, A. Ohara, P.K. Okuro, J.G. dos Santos, R. P. Brexo, H.H. Sato, Whey protein as a key component in food systems: Physicochemical properties, production technologies and applications, *Food Structure* 14 (2017) 17–29, <https://doi.org/10.1016/j.foosr.2017.05.004>.
- [4] B. Mann, A. Kumari, R. Kumar, R. Sharma, K. Prajapati, S. Mahboob, S. Athira, Antioxidant activity of whey protein hydrolysates in milk beverage system, *J. Food Sci. Technol.* 52 (6) (2015) 3235–3241, <https://doi.org/10.1007/s13197-014-1361-3>.
- [5] D.H.G. Pelegrine, C.A. Gasparetto, Whey proteins solubility as function of temperature and pH, *LWT-Food Sci. Technol.* 38 (1) (2005) 77–80, <https://doi.org/10.1016/j.lwt.2004.03.013>.
- [6] C. Ozuna, I. Paniagua-Martínez, E. Castaño-Tostado, L. Ozimek, S.L. Amaya-Llano, Innovative applications of high-intensity ultrasound in the development of functional food ingredients: Production of protein hydrolysates and bioactive peptides, *Food Res. Int.* 77 (2015) 685–696, <https://doi.org/10.1016/j.foodres.2015.10.015>.
- [7] A. Dryakova, A. Pihlanto, P. Marnila, L. Curda, H.J. Korhonen, Antioxidant properties of whey protein hydrolysates as measured by three methods, *Eur. Food Res. Technol.* 230 (6) (2010) 865–874, <https://doi.org/10.1007/s00217-010-1231-9>.
- [8] R. Adjonu, G. Doran, P. Torley, S. Agboola, Screening of whey protein isolate hydrolysates for their dual functionality: Influence of heat pre-treatment and enzyme specificity, *Food Chem.* 136 (3–4) (2013) 1435–1443, <https://doi.org/10.1016/j.foodchem.2012.09.053>.
- [9] L. Grosu, B. Fernandez, C.G. Grigoras, O.I. Patriciu, I.C. Grig-Alexa, D. Nicuță, D. Ciobanu, L. Gavrilă, A.L. Finaru, Valorization of whey from dairy industry for agricultural use as fertiliser: effects on plant germination and growth, *Environ. Eng. Manage. J.* 11 (12) (2012) 2203–2210.
- [10] M. Cappelletti, M. Perazzoli, A. Nesler, O. Giovannini, I. Pertot, The effect of hydrolysis and protein source on the efficacy of protein hydrolysates as plant resistance inducers against powdery mildew, *J. Bioprocess. Biotechniques* 7 (5) (2017), <https://doi.org/10.4172/2155-9821.1000306>.
- [11] C.R. Holkar, A.J. Jadhav, P.S. Bhavsar, S. Kannan, D.V. Pinjari, A.B. Pandit, Acoustic cavitation assisted alkaline hydrolysis of wool based keratins to produce organic amendment fertilizers, *ACS Sustainable Chem. Eng.* 4 (5) (2016) 2789–2796, <https://doi.org/10.1021/acssuschemeng.6b00298>.
- [12] N. Eslahi, F. Dadashian, N.H. Nejad, Optimization of enzymatic hydrolysis of wool fibers for nanoparticles production using response surface methodology, *Adv. Powder Technol.* 24 (1) (2013) 416–426, <https://doi.org/10.1016/j.apt.2012.09.004>.
- [13] S.S. Arya, O. Sawant, S.K. Sonawane, P.L. Show, A. Waghmare, R. Hilares, J.C. D. Santos, Novel, nonthermal, energy efficient, industrially scalable hydrodynamic cavitation—Applications in food processing, *Food Rev. Int.* 1–24 (2019), <https://doi.org/10.1080/87559129.2019.1669163>.
- [14] C.R. Holkar, A.J. Jadhav, D.V. Pinjari, A.B. Pandit, Cavitationally driven transformations: A technique of process intensification, *Ind. Eng. Chem. Res.* 58 (15) (2019) 5797–5819, <https://doi.org/10.1021/acs.iecr.8b04524>.
- [15] S.B. Doltade, G.G. Dastane, N.L. Jadhav, A.B. Pandit, D.V. Pinjari, N. Somkuwar, R. Paswan, Hydrodynamic cavitation as an imperative technology for the treatment of petroleum refinery effluent, *J. Water Process Eng.* 29 (2019), 100768, <https://doi.org/10.1016/j.jpwe.2019.02.008>.
- [16] A.R. Salve, K. Pegu, S.S. Arya, Comparative assessment of high-intensity ultrasound and hydrodynamic cavitation processing on physico-chemical properties and microbial inactivation of peanut milk, *Ultrason. Sonochem.* 59 (2019), 104728, <https://doi.org/10.1016/j.ulsonch.2019.104728>.
- [17] F. Yang, X. Liu, X.E. Ren, Y. Huang, C. Huang, K. Zhang, Swirling cavitation improves the emulsifying properties of commercial soy protein isolate, *Ultrason. Sonochem.* 42 (2018) 471–481, <https://doi.org/10.1016/j.ulsonch.2017.12.014>.
- [18] S. Chakraborty, C. Shrivastava, Comparison between multiresponse-robust process design and numerical optimization: A case study on baking of fermented chickpea flour-based wheat bread, *J. Food Process Eng.* 42 (3) (2019) 13008, <https://doi.org/10.1111/jfpe.13008>.
- [19] V.B. Veljkovic, A.V. Velickovic, J.M. Avramovic, O.S. Stamenkovic, Modeling of biodiesel production: performance comparison of Box-Behnken, face central composite and full factorial design, *Chin. J. Chem. Eng.* 27 (7) (2019) 1690–1698, <https://doi.org/10.1016/j.cjche.2018.08.002>.
- [20] A.B. Muley, A.S. Thorat, S.G. Dalvi, M.I. Talib, V.R. Parate, Comparative studies and correlation between physicochemical and functional properties of chitosan from marine sources, *Trends Biosci.* 22 (8) (2015) 6267–6274.
- [21] N.T. Hoyle, J. Merritt, Quality of fish protein hydrolysates from herring (*Clupea harengus*), *J. Food Sci.* 59 (1) (1994) 76–79, <https://doi.org/10.1111/j.1365-2621.1994.tb06901.x>.
- [22] O.H. Lowry, N.J. Rosebrough, A.L. Farr, R.J. Randall, Protein measurement with the Folin phenol reagent, *J. Biol. Chem.* 193 (1951) 265–275.
- [23] A.B. Muley, S.A. Chaudhari, K.H. Mulchandani, R.S. Singhal, Extraction and characterization of chitosan from prawn shell waste and its conjugation with cutinase for enhanced thermo-stability, *Int. J. Biol. Macromol.* 111 (2018) 1047–1058, <https://doi.org/10.1016/j.ijbiomac.2018.01.115>.
- [24] U.K. Vijayan, S. Varakumar, R.S. Singhal, A comparative account of extraction of oleoresin from *Curcuma aromatica* Salisb by solvent and supercritical carbon dioxide: Characterization and bioactivities, *LWT* 116 (2019), 108564, <https://doi.org/10.1016/j.lwt.2019.108564>.
- [25] A. Waghmare, K. Nagula, A. Pandit, S. Arya, Hydrodynamic cavitation for energy efficient and scalable process of microalgae cell disruption, *Algal Res.* 40 (2019), 101496, <https://doi.org/10.1016/j.algal.2019.101496>.
- [26] X. Mao, Y. Hua, Composition, structure and functional properties of protein concentrates and isolates produced from walnut (*Juglans regia* L.), *Int. J. Mol. Sci.* 13 (2012) 1561–1581, <https://doi.org/10.3390/ijms13021561>.
- [27] Fohely, F., Suardi, N. (2018). Study the characterization of spectral absorbance on irradiated milk protein. In *Journal of Physics: Conference Series* (Vol. 995, No. 1, p. 012056). IOP Publishing.
- [28] M.B. Arnao, Some methodological problems in the determination of antioxidant activity using chromogen radicals: A practical case, *Trends Food Sci. Technol.* 11 (2000) 419–421, [https://doi.org/10.1016/S0924-2244\(01\)00027-9](https://doi.org/10.1016/S0924-2244(01)00027-9).
- [29] W. Wang, E.G. De Mejia, A new frontier in soy bioactive peptides that may prevent age-related chronic diseases, *Compr. Rev. Food Sci. Food Saf.* 4 (4) (2005) 63–78, <https://doi.org/10.1111/j.1541-4337.2005.tb00075.x>.
- [30] S.K. Sonawane, S.S. Arya, Bioactive *L. acidissima* protein hydrolysates using Box-Behnken design, *Biotech* 7 (3) (2017) 218, <https://doi.org/10.1007/s13205-017-0862-y>.
- [31] B. Kong, Y.L. Xiong, Antioxidant activity of zein hydrolysates in a liposome system and the possible mode of action, *J. Agric. Food. Chem.* 54 (16) (2006) 6059–6068, <https://doi.org/10.1021/jf060632q>.
- [32] M. Iskandar, L. Lands, K. Sabally, B. Azadi, B. Meehan, N. Mawji, C. Skinner, S. Kubow, High hydrostatic pressure pretreatment of whey protein isolates improves their digestibility and antioxidant capacity, *Foods* 4 (2) (2015) 184–207, <https://doi.org/10.3390/foods4020184>.
- [33] S. Nardi, D. Pizzeghello, M. Schiavon, A. Ertani, Plant biostimulants: Physiological responses induced by protein hydrolyzed-based products and humic substances in plant metabolism, *Scientia Agricola* 73 (1) (2016) 18–23, <https://doi.org/10.1590/0103-9016-2015-0006>.
- [34] G. Colla, Y. Roupael, R. Canaguier, E. Svecova, M. Cardarelli, Biostimulant action of a plant-derived protein hydrolysate produced through enzymatic hydrolysis, *Front. Plant Sci.* 5 (2014) 448, <https://doi.org/10.3389/fpls.2014.00448>.
- [35] P.S. Shingote, P.G. Kwar, M.C. Pagariya, A.B. Muley, K.H. Babu, Isolation and functional validation of stress tolerant *EaMYB18* gene and its comparative physico-biochemical analysis with transgenic tobacco plants overexpressing *SoMYB18* and *SSMYB18*, *Biotech* 10 (5) (2020) 225, <https://doi.org/10.1007/s13205-020-02197-2>.
- [36] A.B. Muley, M.R. Ladole, P. Suprasanna, S.G. Dalvi, Intensification in biological properties of chitosan after  $\gamma$ -irradiation, *Int. J. Biol. Macromol.* 131 (2019) 435–444, <https://doi.org/10.1016/j.ijbiomac.2019.03.072>.
- [37] A.B. Muley, P.R. Shingote, A.P. Patil, S.G. Dalvi, P. Suprasanna, Gamma radiation degradation of chitosan for application in growth promotion and induction of stress tolerance in potato (*Solanum tuberosum* L.), *Carbohydr. Polym.* 210 (2019) 289–301, <https://doi.org/10.1016/j.carbpol.2019.01.056>.
- [38] A. Nurdiawati, C. Suherman, Y. Maxiselvi, M.A. Akbar, B.A. Purwoko, P. Prawisudha, K. Yoshikawa, Liquid feather protein hydrolysate as a potential fertilizer to increase growth and yield of patchouli (*Pogostemon cablin* Benth) and mung bean (*Vigna radiata*), *Int. J. Recycl. Organ. Waste Agricult.* 8 (2019) 221, <https://doi.org/10.1007/s40093-019-0245-y>.
- [39] S. Trevisan, A. Manoli, S. Quaggiotti, A novel biostimulant, belonging to protein hydrolysates, mitigates abiotic stress effects on maize seedlings grown in hydroponics, *Agronomy* 9 (1) (2019) 28, <https://doi.org/10.3390/agronomy9010028>.
- [40] A. Ertani, S. Nardi, O. Francioso, S. Sanchez-Cortes, M. Di Foggia, M. Schiavon, Effects of two protein hydrolysates obtained from chickpea (*Cicer arietinum* L.) and *Spirulina platensis* on *Zea mays* (L.) plants, *Frontiers, Plant Sci.* 10 (2019) 954, <https://doi.org/10.3389/fpls.2019.00954>.